Journal of Solid State Chemistry **166,** 142–147 (2002)
doi:10.1006/jssc.2002.9571, available online at http://www.idealibrary.com on IDEAL®

Charge Generation in a Dye-Sensitized Solid-State Cell under Different Modes of Illumination

P. M. Sirimanne,[1,2] T. Shirata, T. Soga,[1] and T. Jimbo

Department of Environmental Technology and Urban Planning, Nagoya Institute of Technology, Gokiso-cho, Showa Ku, Nagoya 466-8555, Japan

Received November 11, 2001; in revised form February 19, 2002; accepted March 1, 2002

A dye-sensitized solid-state cell was fabricated by sandwiching ruthenium bypridyl complex in between porous TiO_2 and CuI films. Cis-dithiocyanate-bis(2,2′-bipyridyl -4-4′-dicarboxylate) ruthenium (II) exhibited excellent performance among the dyes tested for TiO_2|dye|CuI cell. Different mechanisms are proposed for charge generation of the cell under different modes of illumination. A high incident photon to current conversion efficiency was observed under back wall illumination compared to that of front wall illumination. Dye molecules exhibited a relay effect under back wall mode illumination at wavelengths shorter than 400 nm. © 2002 Elsevier Science (USA)

Key Words: **microporous TiO_2 films; CuI; dye-sensitized solid-state cell; modes of illumination; relay effect.**

1. INTRODUCTION

In recent years, dye-sensitized systems have aroused much attention as a cheap alternative source for regenerative power sources. The dye-sensitization process on wide band gap semiconductors was investigated in the 1960s (1). Since then rapid development of this field has to be seen. The dye-sensitized nano-porous TiO_2 cell fabricated by Gratzel and co-workers was the breakthrough of dye-sensitized photoelectrochemical cells (2). In dye-sensitized photoelectrochemical cells, dye molecules are photoexcited from the singlet to the excited state and electrons are injected into the conduction band of the semiconductor in an anodic sensitization. Thereby, dye cations are generated. The positive charge of the dye cation is scavenged by one-half of the redox couple present in the electrolyte. The liquid electrolyte in dye-sensitized photoelectrochemical cells presents several technological problems such as dye desorption, solvent vaporization, seal imperfection, reaction of the sealant with the electrolyte and reaction other than those of the redox cycle (3, 4). The above problems can be circumvented when the liquid electrolyte is replaced with a wide band gap transparent hole collector or p-type semiconductor. For the first time, concept of dye-sensitized solid-state cells was reported by Tennakone *et al.* in 1988 (5). One of the authors of this paper (PMS) and collaborators developed dye-sensitized solid-state cell by replacing liquid electrolyte with wide band gap p-CuI, band gap = 3.1 eV (6). The solid-state dye-sensitized photovoltaic n-TiO_2|Cyanadin|p-CuI cell gave a short-circuit photocurrent of about 2.5 mA cm^{-2} and an open-circuit voltage of about 370 mV for simulated sunlight (800 Wm^{-2}). The energy conversion efficiency of the cell was about 1%. The sensitizers that yield highest recorded quantum efficiencies in dye-sensitized systems are ruthenium bipridyl complexes (7, 8). Recently, a solid-state photovoltaic cell sensitized with a ruthenium complex [*cis*-dithiocyanate-bis(2,2′-bipyridyl-4-4′- dicarboxylate)] ruthenium (II) was fabricated by Tennakone *et al.* in 1998 (9). As far as we know different photoeffects of the TiO_2|dye|CuI cell under front wall mode and back wall mode illuminations have not been studied so far. In the present article, we report different charge injection mechanisms for the TiO_2|dye|CuI cell under different modes of illumination.

2. EXPERIMENT

All chemicals used in this work were as obtained from the suppliers and without any further purification.

2.1. *Deposition of TiO_2 on Conduction Glass Plates*

Glacial acetic acid (5.5 mL), 5 mL of tetraisopropyl titanate $[(CH_3)_2CHO]_4$ (Aldrich) and 1 drop of triton X-100 (Sigma) were mixed with 10 mL of 2 propanol. Water (3 mL) was added to the above solution drop wise while vigorously stirring the solution. TiO_2 powder (0.65 g, Nihon Aerisol) was added to the above mixture and was kept under vigorous stirring for 2–3 h. The resulting semi-colloidal suspension was used as the stock solution. A small amount of the stock solution was spread on preheated (at about 150°C)

---

[1] Please address correspondence to P.M. Sirimanne (psirimanne@hotmail.com) and T. Soga (soga@elcom.nitech.ac.jp). Fax: 81-52-735-7120.

[2] Also at Semiconductor Laboratory, Toyota Technological Institute, 2-12-1 Hisakata, Tempaku, Nagoya 468-8511, Japan.

0022-4596/02 $35.00

fluorine-doped conduction glass plate ($1 \times 2.5\ cm^2$) by plastic dropper and was allowed to dry for few minutes. TiO_2-coated glass plate was fired at 450°C for 30 min. Loose crust was removed by wiping smoothly TiO_2 film by cotton wool. The thickness of the TiO_2 film was successively controlled by repeating the coating procedure. Finally, TiO_2-coated conducting glass plates were cleaned by washing with acetonitrile. Thickness of the TiO_2 film was measured with a surface profiler (Alpha-step 500).

2.2. Dye-Coating Procedure on TiO_2 Film

Dye was coated on TiO_2 electrodes as follows: TiO_2-coated glass plates were kept immersed in the dye solution (0.5 mg/L in dry ethanol) and the temperature of the dye solution was maintained at 40°C. Dye-coating process was carried in an oil bath. The dye concentration on the TiO_2 electrodes was controlled by varying immersion time in the dye solution. Dye-coated TiO_2 plates were cleaned by boiling with acetonitrile under low flame. The amount of dye attached to the surface of TiO_2 electrode was estimated by extracting the dye into a basic alcoholic solution. *cis*-dithiocyanate-bis (2,2′- bipyridyl-4-4′-di-carboxylate) ruthenium (II) and tris(2,2′-bipyridyl-4-4′-dicarboxylate) ruthenium (II) were used as the dyes.

2.3. CuI-Coating Procedure on Dyed TiO_2 Film

CuI (0.6 g Nacalai tesque) was mixed with 15 mL of moisture-free acetonitrile and was allowed to precipitate excess CuI. The filtrate was separated. A small amount of methyl 3 ethyl imidazolium thiocyanate was added to the solution as a surfactant. A small amount of the above solution was carefully spread on the surface of dye-coated TiO_2 plate and heated at 150°C. This procedure was repeated until the conductivity of the CuI film reaches $50\ \Omega\,cm^{-1}$.

2.4. Measurements

Transmittance spectra of CuI, TiO_2 films and absorption spectra of dye solutions were measured by using UV|VIS|NIR spectrometer (Jasco V-570). Surface morphology of CuI and TiO_2 films was studied using scanning electron microscope (SEM) (Hitachi S3000H). The cell was constructed by pressing a Pt-coated glass plate (transparency $> 90\%$ for visible light) on the CuI|dye|TiO_2 electrode. Photoeffects of the cell were studied by illuminating the cell through TiO_2 layer (back wall mode illumination) and CuI layer (front wall illumination). The variation of incident photon to current conversion efficiency of the cell with wavelength was measured using monochromator (Jasco) coupled with single-phased lock-in amplifier (NF Instrument-5600 A), under constant photon energy illumination mode ($50\ \mu W\,cm^{-2}$). Current–voltage characteristics were recorded with a solar simulator (Wacom) coupled with semiconductor parameter analyzer (Hewlett Packard HP 4145B), under 1.5 AM condition. Scan speed was $0.01\ V\,min^{-1}$.

3. RESULTS AND DISCUSSION

3.1. General Properties of TiO_2 and CuI Films

TiO_2 films prepared as described above exhibited high degree of porosity and transparency to visible light. Images (a) and (b) in Fig. 1 show scanning electron micrographs of TiO_2 films (a) without and (b) with the addition of Degusa P-25 TiO_2 powder. As observed from the scanning electron micrograph, fractural structure was observed for the samples prepared without the addition of Degusa P-25 TiO_2 powder. Samples prepared by adding Degusa P-25 TiO_2 powder exhibited good interconnection among the large TiO_2 clusters by small interconnected grains. The average thickness of the TiO_2 film was evaluated from SEM by rotating the sample table vertically 90° from its normal position. As observed from the SEM, the average thickness of the TiO_2 film is about 10 μm. This value agrees with the value obtained from direct measurement from a thickness meter (Surface profiler). SEM image of CuI layer is shown in image (c) in Fig. 1. This image clearly indicates that CuI clusters are composed of closely packed small grains. Figure 2 illustrates transmission spectra of (a) CuI and (b) TiO_2 films. These films were coated on quart substrates. The average transmittance is above 70% in the range of wavelength from 900 to 400 nm and reflectance is less than 7% for both films in the wavelength region 300–900 nm. Therefore, most of the light incident on the cell generates current by exciting dye molecules absorbed onto the TiO_2 film or the CuI film. Since most visible light transmits through CuI and TiO_2 layers, the sandwiched dye layer of the cell can easily be illuminated through the CuI layer (front wall mode illumination) or the TiO_2 layer (back wall mode illumination).

3.2. Photoproperties of TiO_2/dye/CuI Cell

TiO_2|CuI cell was fabricated by depositing CuI on a TiO_2 electrode. Only a feeble photoresponse was observed for the TiO_2|CuI cell. We have used two ruthenium dyes to fabricate the TiO_2|dye|CuI cell. Absorbance spectra of used dyes (a) tris (2,2′-bipyridyl-4-4′-dicarboxylate) ruthenium (II) and (b) *cis*-dithiocyanate-bis (2,2′- bipyridyl-4-4′-dicarboxylate) ruthenium (II) are shown in Fig. 3. Only *cis*-dithiocyanate -bis (2,2′- bipyridyl-4-4′-dicarboxylate) ruthenium (II) exhibited excellent performance for the TiO_2|dye|CuI cell. Therefore, this dye was chosen as the sensitizer. The TiO_2|dye|CuI cell was illuminated under front and back modes of illumination. Significantly enhanced photocurrent was observed under both modes of

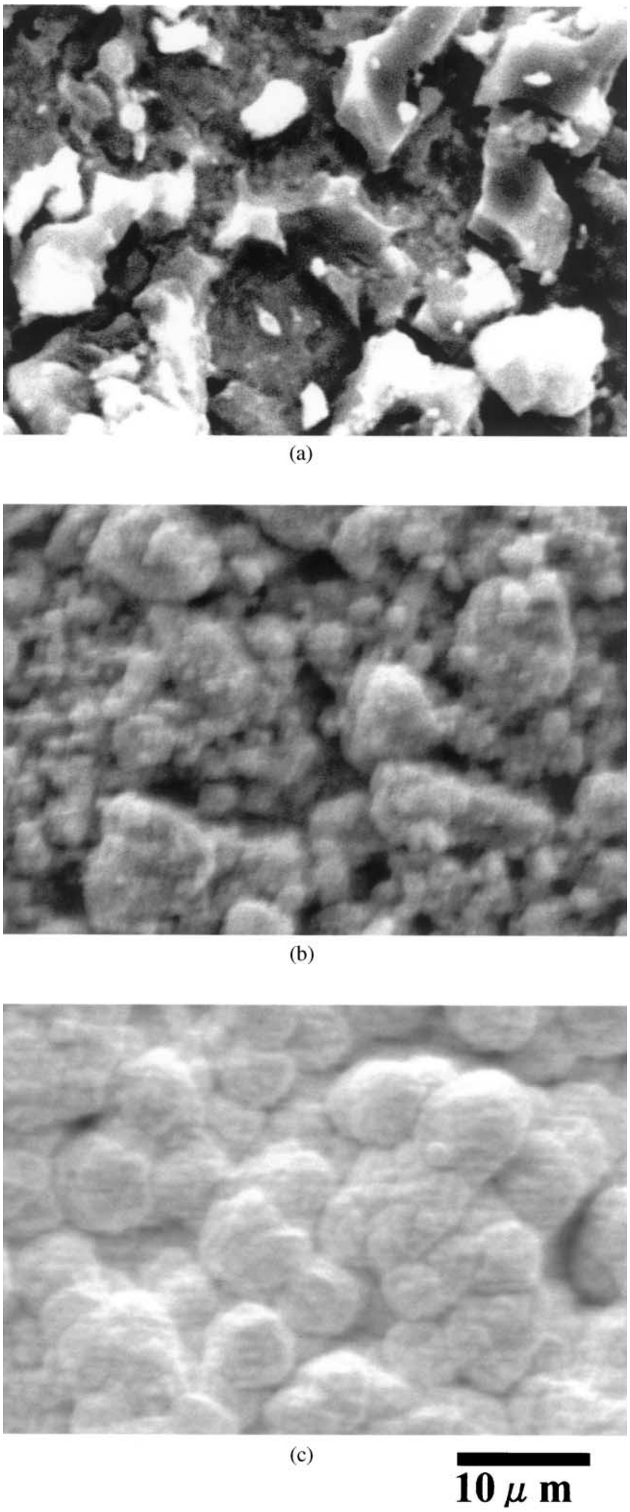

FIG. 1. Scanning electron micrograph of sintered TiO_2 film: (a) without and (b) with TiO_2 P-25 Degusa powder. (c) Scanning electron micrograph of CuI film.

illumination. Action spectra of the TiO_2|dye|CuI cell under front wall and back wall modes are shown as curves (a) and (b) in Fig. 4, respectively. High incident photon to current conversion efficiency over 70% was observed under back wall illumination, as shown in Fig. 4. The value of IPCE for the same cell under front wall mode was about only one-half to that of back wall illumination. This phenomenon cannot be explained from the properties of transmittance of the CuI and TiO_2 films (Fig. 2). It seems to be that some other factors might be involved with the observed high IPCE under back wall mode illumination than that of front wall mode illumination. It has been reported that ruthenium complexes chelate with Ti^{+4} ions via the carboxyl groups of ruthenium dyes and efficient charge injection takes place via these bonds (10). The nature of interaction between CuI and ruthenium dyes has not been reported so far. Charge generation and separation of TiO_2|dye|CuI cell are two-fold and can be summarized as follows:

Upon illumination dye molecules (D) get excited from the ground state to the excited state. D* donates excited dye molecules:

$$D + h\nu \rightarrow D^*. \qquad [1]$$

Electrons are injected from the excited dye molecules to the conduction band of TiO_2:

$$D^* \rightarrow D^+ + e^- \text{ (Conduction band of } TiO_2\text{)}. \qquad [2]$$

The resulting dye cation reaches its ground state by capturing an electron from CuI. Thereby, a hole is created in the valence band of CuI:

$$D^+ \rightarrow D + h^+ \text{ (Valence band of CuI)}. \qquad [3]$$

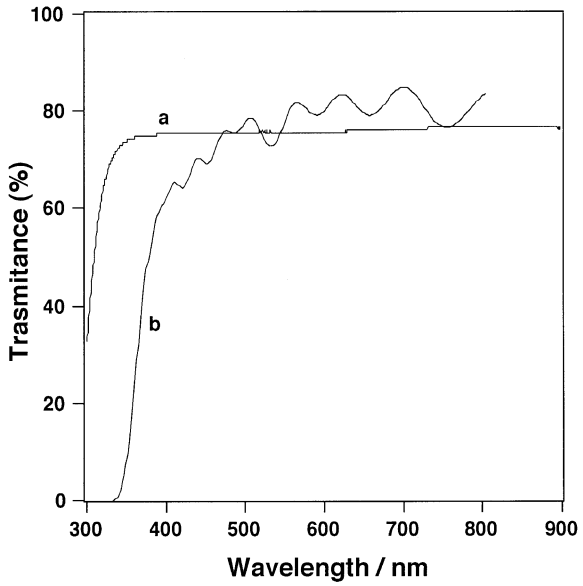

FIG. 2. Transmission spectra of (a) CuI film and (b) TiO_2 film, films were deposited on quart substrates.

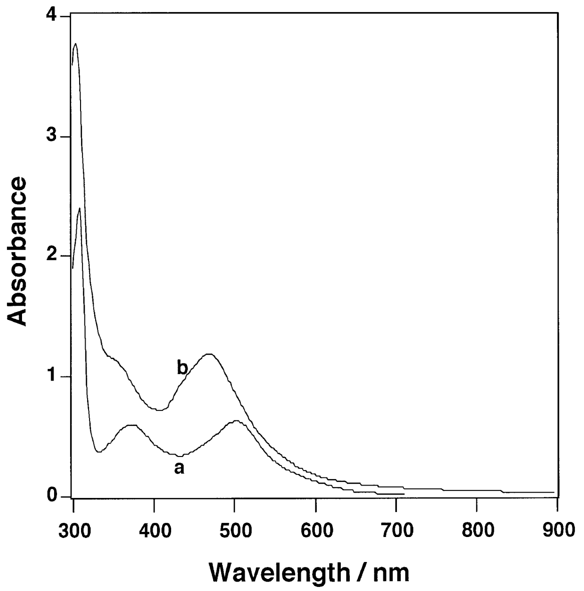

FIG. 3. Absorption spectra of (a) *cis*-dithiocanate-bis(2,2′-bipyridyl-4-4′-di-carboxylate) ruthenium (II) and (b) tris(2,2′-bipyridyl-4-4′-dicarboxylate) ruthenium (II).

This mechanism is directly parallel to the mechanism of charge generation of the "Gratzel cell." In addition to the above processes, excited dye molecules can reach ground state via forming dye cations. This process is similar to that of cathodic sensitization (11) of p-type semiconductor.

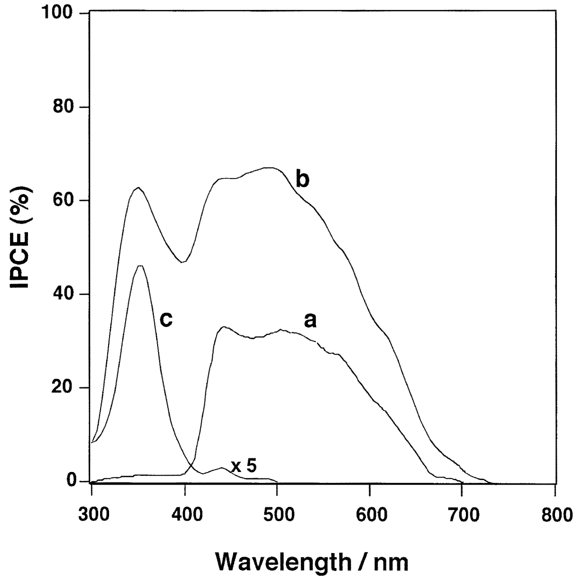

FIG. 4. Variation of incident photon to current conversion efficiency with wavelength of CuI|dye|TiO_2 cell for different modes of illumination: (a) front wall mode and (b) back wall mode. (c) IPCE action spectrum of TiO_2 electrode in aqueous 0.1 M NaOH under illumination. Electrode was biased positively at 0.1 V vs Ag|AgCl.

Dye molecules obtain electrons from the valence band of CuI by generating holes in the valence band:

$$D^* \rightarrow D^- + h^+ \text{ (Valence band of CuI).} \qquad [4]$$

The dye anions reach their ground state by injecting electrons to the conduction band of TiO_2 film:

$$D^- \rightarrow D + e^- \text{ (Conduction band of } TiO_2\text{).} \qquad [5]$$

Steps [2]–[5] govern the amplitude of photocurrent of the cell under illumination. Less photocurrent was observed for the CuI electrodes sensitized with the ruthenium dye compared to that of the value reported for CuI electrode sensitized with methyl violet (12). These results indicate that charge transfer processes between D^- ions and CuI, TiO_2 films (steps [4] and [5]) are fairly favorable in the TiO_2|dye|CuI cell. Photoeffects of thin films of semiconductors have been studied under by illuminating the electrode through semiconductor film and electrolyte. For example, Lindquist *et al.* and Lui *et al.* studied the photoeffects on TiO_2 and CdSe electrodes by illuminating the electrode through semiconductor film and electrolyte (13, 14). An efficient charge generation was observed close to back contact for both electrodes. This effect was pronounced with increasing film thickness. However, the present case is different from those cases because the dye is sandwiched between two semiconductors and also due to the absence of electrolyte. The detailed mechanism for high IPCE under back wall mode to that of front wall mode is not so clear, at present. The actual process of the cell can be summarized as

$$D + h\nu \rightarrow D + e^- \text{ (CB of } TiO_2\text{)} + h^+ \text{ (VB of CuI).} \qquad [6]$$

In addition to the sensitization process, band gap excitation of TiO_2 was observed only under back wall illumination (curve b), as shown in Fig. 4. For comparison, the IPCE action spectrum of TiO_2 electrode is shown in the same figure (curve c). We did not observe any evidence for the band gap excitation of CuI under front wall mode illumination. The high absorption co-efficient of CuI at shorter wavelengths is attributed to the high degree of recombination of photogenerated electrons and holes in CuI clusters. The high degree of recombination of photogenerated charge carriers in CuI clusters may be a reason for the suppression of photocurrent at shorter wavelengths ($\lambda < 400$ nm), under front wall illumination, as shown by curve a in Fig. 4. It has been reported that diffusion-controlled charge transfer between colloidal semiconductor particles in microporous electrodes also strongly affects the photocurrent of the system (15–17). Different rates of diffusion-controlled charge transfer between TiO_2 particles and CuI particles may be another reason for the difference between IPCE action spectra under front wall mode and back wall mode illuminations (graphs a, b in Fig. 4). The charge generation of the cell due to band gap excitation of TiO_2 under back wall illumination is shown in Fig. 5. The photocurrent

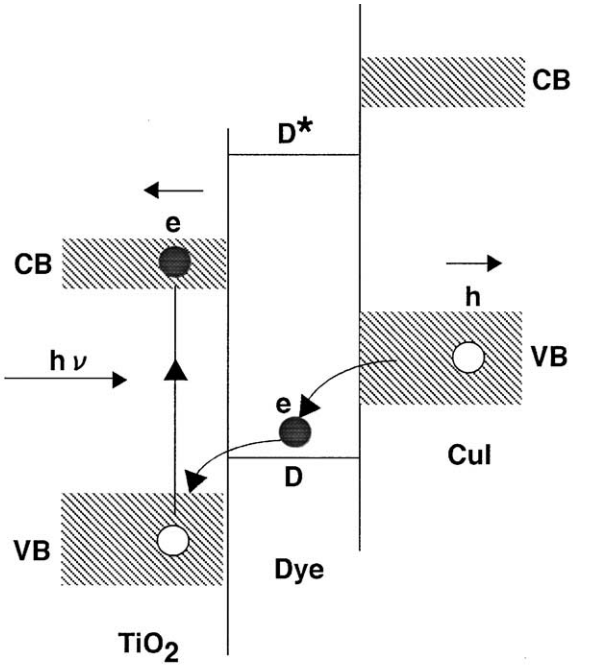

FIG. 5. Charge generation of the CuI|dye|TiO_2 cell under back wall mode illumination with wavelengths shorter than 400 nm.

generation due to band gap excitation of TiO_2 can be summarized as follows:

Excitation of TiO_2 under back wall mode illumination:

$$TiO_2 + h\nu \rightarrow e^- \text{ (CB of } TiO_2) + h^+ \text{ (VB of } TiO_2). \quad [7]$$

Photogenerated holes obtain electrons from CuI and thereby holes are transmitted to the CuI film. Intermediate steps can be summarized as follows:

Electron transfer step from dye molecules to the valence band of TiO_2:

$$h^+ \text{ (Valence band of } TiO_2) + D \rightarrow D^{+\cdot} \quad [8]$$

The generated hole is transmitted through the dye molecules and neutralize by obtaining an electron from CuI.

Electron transfer step from the valence band of CuI to dye cation:

$$D^+ \rightarrow D + h^+ \text{ (Valence band of CuI)}. \quad [9]$$

The location of conduction band of TiO_2, ground state of dye molecules and the valence band of CuI permits the above charge transfer process energetically. Here, dye molecules behave as a mediator. The relay effect of dye molecules in the dye-sensitized systems by dye molecules has been reported (18, 19). However, net process of the cell can be summarized as follows:

$$TiO_2 + h\nu \rightarrow e^- \text{ (CB of } TiO_2) + h^+ \text{ (VB of CuI)}. \quad [10]$$

IPCE action spectra of TiO_2|dye|CuI cell for different concentrations of dye, under back wall mode illumination are shown in Fig. 6. The curves c, b and a represent the surface concentration of the dye on the electrode in descending order. Photocurrent of the cell due to band gap excitation of TiO_2 increases with increasing coverage of dye on the TiO_2 electrode and then decreases with further increasing coverage of the dye. Sensitized photocurrent of the cell also followed similar pattern. Similar pattern was observed in dye-sensitized systems earlier [18]. Loss of energy due to quenching of excited dye molecules might be a reason for the observed low IPCE at high dye concentrations on the electrode. The stability of the photocurrent was studied under different intensities of illumination. Almost constant photocurrent was observed for low light intensities (5 mW cm^{-2}). However, a decay of the photocurrent of about 5% h^{-1} was observed under illumination with AM 1.5. The stability of the photocurrent was increased when the UV light is filtered. This result indicates UV degradation of the dye molecules as well as TiO_2 and CuI responsible for the decay of the photocurrent of the cell. We have obtained a maximum short-circuit photocurrent of 10–12 mA cm^{-2} and an open-circuit voltage of 470 mV for the TiO_2|dye|CuI cell under AM 1.5 conditions. Current–voltage characteristic of the cell under back wall illumination are shown in Fig. 7. Power conversion efficiency and the fill factor of the cell are about 2.75% and 0.4, respectively. Undoubtedly, these cell parameters are rather low. Cell parameters would further improve by choosing appropriate methods to deposit CuI and avoiding short-circuiting of the charge carriers of the cell.

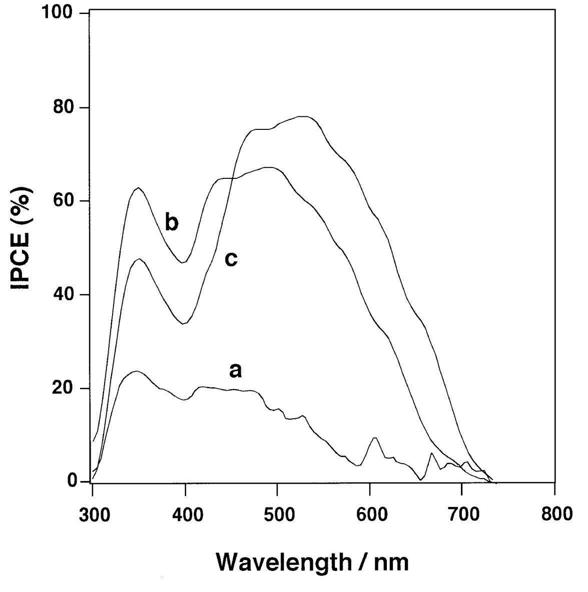

FIG. 6. Variation of incident photon to current conversion efficiency with wavelength of CuI|dye|TiO_2 cell for different monolayers of dye at the surface, under back wall mode illumination, where SC_{dye} is the concentration of dye on the electrode: $SC_{dye,c} > SC_{dye,b} > SC_{dye,a}$.

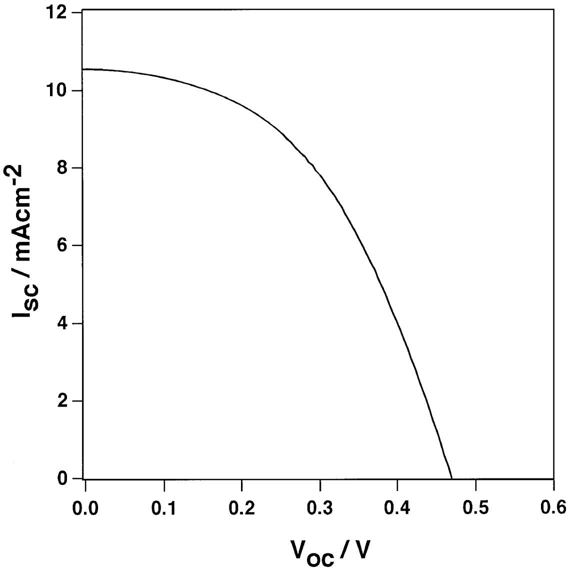

FIG. 7. Current–voltage characteristics of CuI|dye|TiO_2 cell. The scanning speed was 0.01 V min^{-1}.

4. CONCLUSION

A dye-sensitized solid-state cell was fabricated by using cheap materials. It was found that addition of TiO_2 powder (P-25 Degusa) to the hydrolysis solution of titanium isopropoxide increases the photoactivity of the cell. The rate of the charge transfer process between Ti^{+4} ions and dye molecules is the key factor, which governs the cell performance. Among the dyes tested for the study *cis*-dithiocyanate-bis(2,2′- bipyridyl-4-4′-dicarboxylate) ruthenium (II) gave the highest performance for the cell. Enhancement of IPCE was observed under back wall illumination to that of front wall mode illumination. Adsorbed dye molecules to the TiO_2 surface act as a relay, specially under back wall illumination in the wavelength region of 300–400 nm.

ACKNOWLEDGMENTS

Discussion with Prof. K. Tennakone and Dr. G.R.A. Kumara was greatly appreciated by one of the authors PMS.

REFERENCES

1. H. Gerischer and H. Tributsch, *Ber. Bunsenges. Phys. Chem.* **72,** 437 (1968).
2. B. O'Regan and M. Gratzel, *Nature* **353,** 737 (1991).
3. K. Tennakone, G. R. R. A. Kumara, K. G. U. Wijayantha, I. R. M. Kottegoda, V. P. S. Perera, and G. M. L. P. Aponsu, *Semicond. Sci. Technol.* **13,** 134 (1998).
4. K. Tennakone, V. P. S. Perera, I. R. M. Kottegoda, and G. R. R. A. Kumara, *J. Phys. D* **32,** 374 (1999).
5. K. Tennakone, K. P. Hewaparakrama, M. Dewasurendra, A. H. Jayathissa, and L. K. Weerasena, *Semicond. Sci. Technol.* **3,** 382 (1988).
6. K. Tennakone, G. R. R. A. Kumara, A. R. Kumarasinghe, K. U. G. Wijayantha, and P. M. Sirimanne, *Semicond. Sci. Technol.* **10,** 1689 (1995).
7. C. J. Barbe, F. Arendse, P Comte, M. Jirousek, F. Lenzmann, V. Shklover, and M. Gratzel, *J. Am. Ceram. Soc.* **80,** 3157 (1997).
8. A. Mills and S. L. Hunt, *J. Photochem. Photobiol.* **108,** 1 (1997).
9. K. Tennakone, G. R. R. A. Kumara, I. R. M. Kottegoda, and K. G. U. Wijayantha, *J. Phys. D* **31,** 1492 (1998).
10. M. Gratzel and K. Kalyanasundaram, *Curr. Sci.* **66**(10), 706 (1994).
11. N. Mott and R. W. Gurney, *Proc. R. Soc. A* **164,** 151 (1938).
12. K. Tennakone, A. R. Kumarasinghe, and P. M. Sirimanne, *Semicond. Sci. Technol.* **8,** 1557 (1993).
13. S. E. Lindquist, B. Finnstrom, and L. Tegner, *J. Electrochem. Soc.* **130,** 351 (1983).
14. Di Lui and P. V. Kamat, J. *Phys. Chem.* **97,** 10769 (1990).
15. B. O'Regan, J. Moser, M. Anderson, and M. Gratzel, *J. Phys. Chem.* **94,** 8720 (1990).
16. A. Hegfeldt, U. Bjorksten, and S. Lindquist, *Sol. Matter Sol. Cells* **27,** 304 (1992).
17. K. Tennakone, A. R. Kumarasinghe, P. M. Sirimanne, and G. R. R. A. Kumara. *J. Photochem. Photobiol.* **91,** 59 (1995).
18. K. Tennakone, A. R. Kumarasinghe, and P. M. Sirimanne. *J. Photochem. Photobiol.* **88,** 39 (1995).
19. K. Tennakone, G. R. R. A. Kumara, and K. G. U. Wijayantha, *Semicond. Sci. Technol.* **11,** 1737 (1996).